ORIGINAL ARTICLE | OPEN ACCESS

Flagellar Assembly Factor FliW2 De-Represses *Helicobacter pylori* FlaA-Mediated Motility by Allosteric Obstruction of Global Regulator CsrA

Marcia Shu-Wei Su[1,2] | Benjamin Dickins[3] | Fang Yie Kiang[2] | Wei-Jiun Tsai[4] | Yueh-Lin Chen[2] | Jenn-Wei Chen[5] | Shuying Wang[5] | Pei-Jane Tsai[6] | Jiunn-Jong Wu[1,2,7] 🆔

[1]Department of Medical Laboratory Science and Biotechnology, College of Medical and Health Sciences, Asia University, Taichung, Taiwan | [2]Department of Biotechnology and Laboratory Science in Medicine, College of Biomedical Science and Engineering, National Yang Ming Chiao Tung University, Taipei, Taiwan | [3]Department of Biosciences, Nottingham Trent University, Nottingham, UK | [4]Institute of Basic Medical Sciences, College of Medicine, National Cheng-Kung University, Tainan, Taiwan | [5]Department of Microbiology and Immunology, College of Medicine, National Cheng-Kung University, Tainan, Taiwan | [6]Department of Medical Laboratory Science and Biotechnology, College of Medicine, National Cheng Kung University, Tainan, Taiwan | [7]Department of Medical Research, China Medical University Hospital, China Medical University, Taichung, Taiwan

Correspondence: Jiunn-Jong Wu (jjwu1019@asia.edu.tw)

ABSTRACT

Background: *Helicobacter pylori* colonizes the human stomach as a dominant member of the gastric microbiota and constitutively expresses flagellar motility for survival. Carbon storage regulator A (CsrA) is a posttranscriptional global regulator and a critical determinant of *H. pylori*'s motility and pathogenicity. The regulation of *H. pylori* CsrA is still uncertain although in other species CsrA is reported to be antagonized by small RNAs and proteins. In this study, we attempted to unveil how CsrA is regulated and hypothesized that *H. pylori* CsrA activity is antagonized by a flagellar assembly factor, FliW2, via protein allosteric obstruction.

Materials and Methods: Multiple sequence comparisons indicated that, along its length and in contrast to *fliW1*, the *fliW2* of *H. pylori* J99 is conserved. We then generated an isogenic Δ*fliW2* strain whose function was characterized using phenotypic and biochemical approaches. We also applied a machine learning approach (AlphaFold2) to predict FliW2-CsrA binding domains and investigated the FliW2-CsrA interaction using pull-down assays and in vivo bacterial two-hybrid systems.

Results: We observed the reduced expression of major flagellin FlaA and impaired flagellar filaments that attenuated the motility of the Δ*fliW2* strain. Furthermore, a direct interaction between FliW2 and CsrA was demonstrated, and a novel region of the C-terminal extension of CsrA was suggested to be crucial for CsrA interacting with FliW2. Based on our AlphaFold2 prediction, this C-terminal region of FliW2-CsrA interaction does not overlap with CsrA's N-terminal RNA binding domain, implying that FliW2 allosterically antagonizes CsrA activity and restricts CsrA's binding to *flaA* mRNAs.

Conclusions: Our data points to novel regulatory roles that the *H. pylori* flagellar assembly factor FliW2 has in obstructing CsrA activity, and thus FliW2 may indirectly antagonize CsrA's regulation of *flaA* mRNA processing and translation. Our findings reveal a new regulatory mechanism of flagellar motility in *H. pylori*.

1 | Introduction

Gram-negative microaerophilic *Helicobacter pylori* of Epsilonproteobacteria colonizes the human stomach as a dominant member of the gastric microbiota and is a causative agent of gastric infections that may lead to the development of gastroduodenal diseases and gastric cancer [1–3]. Unlike Gammaproteobacteria, which are mostly found in intestinal niches, *H. pylori*'s gastric milieu constitutes a uniquely hostile ecological niche. Because of the restriction of small absorptive nutrients and the acidity of the stomach [4], *H. pylori*'s environment may favor the evolution of multilayered hierarchical regulatory networks [5]. *H. pylori* constitutively expresses flagellar biosynthesis, chemotaxis, and motility as essential housekeeping functions in vivo [6]. Due to the lack of the master regulator FlhDC in the flagellar regulatory network of Epsilonproteobacteria, the biogeneses of flagella in *H. pylori* and *Campylobacter jejuni* are fundamentally different from those of *Escherichia coli* and *Salmonella* (Gammaproteobacteria) [7]. Flagella-mediated motility is one of the crucial virulence determinants and it is tightly regulated. The regulation of the flagellar motility in Epsilonproteobacteria includes three transcriptional sigma factors (RpoD/σ^{80}, RpoN/σ^{54}, and FliA/σ^{28}), regulators (CsrA, FlgR/S, FlhA/F, FlgM, HrcA, and HspR), and small RNAs (CncR1 and FlmE/R) during the early (class I), middle (class II), and late (class III) stages of flagellar biosynthesis, respectively [8–15]. Of these, the global posttranscriptional regulator CsrA (carbon storage regulator A) has been widely studied for its modulation of carbon metabolism, stress responses, virulence, biofilm formation, flagellar biosynthesis, and motility [13, 14, 16–18].

CsrA regulates the expression of downstream genes via mechanisms that operate posttranscriptionally and translationally. When a CsrA dimer binds to NGGA motifs on the leader sequence of a transcript, it can stabilize target mRNAs, promote Rho-dependent transcriptional termination, change RNA secondary structure to repress or activate translation, or occupy the Shine-Dalgarno (SD) sequence to occlude ribosome binding [19]. In *E. coli*, CsrA activates the expression of several motility genes, including the *flhDC* operon that encodes the transcription factor FlhDC for flagellar biosynthesis and chemotaxis [20, 21]. However, studies of CsrA regulation in *Bacillus* and *Campylobacter* show that genes for flagellar filament formation and motility are repressed by CsrA [14, 22]. The regulation of CsrA antagonists in the different species also reveals interesting patterns. In *E. coli* and Gammaproteobacteria, the non-coding small RNAs, CsrB and CsrC, form a secondary structure known as a "hedgehog ball", where many NGGA sequences are presented as CsrA binding sites [23–27]. The CsrB binds to *E. coli* CsrA thus inhibiting the CsrA activity and attenuating the CsrA modulation of gene expression through a competitive antagonism. In addition to small RNA regulation, antagonizing CsrA activity through protein interaction is reported in the cases of enteropathogenic *E. coli* (EPEC), *Bacillus* and *Campylobacter*.

The chaperone CesT required for EPEC to colonize in host intestinal epithelial cells reduces CsrA activity by binding to the RNA binding domain of *E. coli* CsrA as a competitive antagonist [28]. Unlike the mechanism of CesT-CsrA binding, a flagellar assembly factor FliW found in *Bacillus subtilis* and *C. jejuni* employs a three-node negative-feedback regulation between FliW, CsrA, and the major flagellin FlaA homolog of flagellar biosynthesis [14, 29–31]. In *B. subtilis*, FliW proteins spatially bind to the different residues of CsrA required for RNA binding, thus inhibiting CsrA activity through an allosteric noncompetitive mechanism. This FliW-CsrA dimeric interaction strictly controls the intracellular concentration of flagellar filament protein Hag (FlaA homolog) for the homeostasis of flagellar biosynthesis and the maintenance of intracellular architecture [29, 31]. A similar but more complicated FlaA-FliW-CsrA negative-feedback regulatory circuit has been reported in *C. jejuni*. *C. jejuni* CsrA primarily binds flagellar mRNAs and/or their 5′ un-translational regions (UTRs) that repress their RNA processing and translation [14]. *C. jejuni* CsrA binds to the abundant *flaA* mRNA and its UTR that translationally represses *flaA* mRNA. In turn, the CsrA activity is modulated by the *flaA* titration. The concentration of the *flaA* mRNA accordingly controls the expression of other flagellar genes through CsrA-mediated posttranscriptional regulation [14]. More interestingly, *C. jejuni* CsrA activity is also antagonized by FliW proteins, which bind the N-terminal subdomain of FlaA flagellins for optimizing the homeostasis of flagellins [14, 30].

In *H. pylori*, CsrA is shown to maintain full motility and facilitate adaptation to environmental stresses by mediating its effect at the posttranscriptional level [16, 18]. The CsrA regulons include oxidant-induced transcriptional response and heat shock response (*ahpC*, NapA, GroESL, and HspR), virulence, and acid adaptation (*napA*, *cagA*, *vacA*, *fur*, and urease operon) [14]. Loss of *csrA* also impairs flagellar motility. In the non-motile N6 Δ*csrA* and 26695 Δ*csrA* mutant strains, the processing and translation of the elevated *flaA* and *flaB* mRNAs may be influenced by CsrA, in contrast to the reduced *flaA* and *flaB* mRNAs and decreased FlaA/FlaB of the non-motile J99 Δ*csrA* mutant strain [16, 18]. Although CsrA is a critical determinant of gene regulation and flagellar biosynthesis, the regulation of CsrA is uncertain. In this study, we attempted to understand whether *H. pylori* CsrA activity is regulated by protein antagonism and how this mechanism affects *H. pylori* motility. We employed a comparative genomic analysis to identify two *fliW* homologs (*jhp1081*-encoded FliW1 and *jhp1291*-encoded FliW2) from the *H. pylori* J99 genome. We characterized the isogenic Δ*fliW2* mutant strain by phenotypic and biochemical analyses, and determined the FliW2-CsrA interaction using a machine learning approach and an in vivo bacterial two-hybrid system. Our findings revealed the crucial roles of FliW2 in flagellar motility and in de-repression of *H. pylori* motility by allosteric obstruction of posttranscriptional regulator CsrA.

2 | Materials and Methods

2.1 | Bacterial Strains and Inoculation

H. pylori strain J99 was incubated at 37°C under microaerobic conditions (5% O_2, 10% CO_2, 85% N_2). For agar plate culturing, strains were grown on Brucella (BD Biosciences, USA) agar plates supplemented with 10% horse serum (Gibco BRL, Life Technologies, USA) for 32 to 36 h. For liquid culturing, *H. pylori* was inoculated in Brucella broth containing 10% horse serum with a starting optical density at 600 nm of 0.2 optical density units (ODU) using a shaker at a speed of 150 rpm. *H. pylori* cells were collected when bacteria reached mid-log phase (1.5 ODU) or early stationary phase (4.0 ODU) [32]. When needed, 10 µg/mL chloramphenicol (Cm) or 10 µg/mL kanamycin (Km) was added to Brucella medium during inoculation. For *E. coli* inoculation, *E. coli* was grown on Luria-Bertani (LB) (BD Biosciences) agar plates or in broth media at 37°C. If required, 100 µg/mL ampicillin (Amp), Cm (25 µg/mL), or Km (25 µg/mL) were supplemented in LB media. The bacterial strains and plasmids used in this study are described in Table S1.

2.2 | Construction of In-Frame Deletion Δ*fliW2* Mutant of *H. pylori*

An in-frame deletion approach was employed to construct a Δ*fliW2* knockout mutant strain of *H. pylori* J99 (genome accession number: NC_000921.1). We used the genomic DNA (gDNA) of J99 wild-type (WT) strain as a template, along with primers jhp1291(fliW2)-PCR-1-XbaI and jhp1291(fliW2)-PCR-2-BamHI (Table S2) to amplify a ~ 1.5 kb fragment containing *fliW2* and its upstream and downstream flanking sequences. This amplicon was then ligated to *Xba*I/*Bam*HI-cleaved pGEMTeasy to generate pGEMTeasy-fliW2 (Table S1). Next, we applied inverse PCR approach to generate an in-frame deletion of *fliW2* with primers jhp1291(fliW2)-mut-3 and jhp1291(fliW2)-mut*-4, followed by ligation with *Hinc*II-cleaved Cm resistance cassette. The resultant pGEMTeasy::fliW2::Cm (pKO-fliW2) was delivered to *H. pylori* J99 WT strain using natural transformation. After homologous recombination occurred, the Cm-resistant transformants were inoculated for gDNA isolation to validate the deletion of *fliW2* gene. The mutation of the Δ*fliW2* #5 strain was confirmed by Southern blotting and Sanger sequencing analyses. In addition, we performed cDNA-qPCR analysis to rule out polar effect in this Δ*fliW2* mutant strain (Figure S1).

2.3 | RNA Isolation, cDNA Conversion, and cDNA-Quantitative PCR Analysis

Bacterial pellets were collected at 1.5 ODU by centrifugation and preserved in *RNALater* solution (Thermo Fisher Scientific, USA). Total RNAs were extracted using GENEzol TriRNA Bacteria Kit (Geneaid, Taiwan) according to the manufacturer's recommendations. The RNA concentration and its quality were determined using a Nanodrop spectrophotometer (NanoDrop ND-1000, USA) and agarose gel electrophoresis. Subsequently, a total of 0.5 µg RNA was converted to cDNAs using ReverTra Ace qPCR RT Master Mix with gDNA Remover (TOYOBO, Osaka, Japan) according to the manufacturer's protocols. Standard

PCR was performed to ensure that there was no residual gDNA. For cDNA-qPCR analysis, cDNA samples were diluted ten-fold using an elution buffer (50 mM Tris–HCl, pH 8.0). The qPCR reaction was prepared containing diluted cDNA, 2× Fast SYBR Green Master mix (Thermo Fisher Scientific) and qPCR primers (Table S2), followed by execution in a StepOnePlus Real-Time PCR System (Thermo Fisher Scientific). The amplification cycling was set as follows: 95°C for 20 s, followed by 40 cycles of 95°C for 3 s and 60°C for 30 s. Data was collected during the extension step. The melting curve was included for qPCR primer quality control. Relative quantification of gene expression was determined and analyzed using the ABI software and $2^{-\Delta\Delta Ct}$ method [33], compared to *gyrA* Ct value as endogenous gene control.

2.4 | Motility Assay Using Soft Agar Plates

A tip-full of *H. pylori* cells were inoculated by being vertically touched to the surface of soft agar (0.3%) plates (pH 7 and 6; Brucella agar/10% horse serum). After a seven-day incubation, we measured the diameter of the migrated bacteria. The motility of each strain was calculated as mean ± SD from at least three independent experiments. The Δ*flaA* mutant strain serves as a non-motile control.

2.5 | Flagellar Filament Examination Using Scanning Electron Microscopy

The grown *H. pylori* J99 WT, Δ*flaA*, and Δ*fliW2* strains were diluted in Brucella broth containing 2% horse serum to have an initial OD_{600} of 0.2. Next, we transferred 1.5 mL of diluted *H. pylori* cells to 24-well plates, which contained lysine-coated glass coverslips. After 30 to 60 h of inoculation under microaerophilic conditions at 37°C, the supernatants were discarded, and the cells were fixed with 2.5% glutaraldehyde in PBS buffer at 4°C for overnight. Fixed cells were washed twice in PBS buffer, and dehydrated by adding 1 mL of ethanol in water in increasing concentration of 70%, 85%, 95%, and 100% (v/v) at room temperature for 10 min. An additional two dehydrations were conducted using 100% ethanol for 15 min for each time, followed by a critical point drying at the Electron Microscopy Facility (National Yang Ming Chiao Tung University). The coverslips containing the adherent cells were immediately coated with Au/Pd on a sputter coater. The examination was performed using a field emission scanning electron microscope (Jeol JSM-7600F, Japan) at an acceleration voltage of 5 kV. The micrographs were taken from at least two different fields from two independent experiments.

2.6 | Generation of Mouse Polyclonal Anti-FlaA and Anti-FliW2 Sera

We over-expressed and purified recombinant FlaA and FliW2 proteins from *E. coli* BL21 harboring pET29b-FlaA and pET22b-FliW2 (Table S1), respectively, according to the recommendations from the manufacturer (Sigma-Aldrich, USA). One hundred micrograms of purified recombinant FlaA and FliW2 proteins were mixed with complete Freund's adjuvant (1:1, v/v),

and subcutaneously injected into female C57BL/6 mice (six to eight-week-old). Mice were boosted three times biweekly for 6 weeks. In the seventh week, the sera were collected from the immunized mice and stored at −20°C.

2.7 | SDS-PAGE and Western Blotting Analysis

Total proteins of collected *H. pylori* cells were extracted and subjected to 10% SDS-PAGE. In brief, after transferring proteins to PVDF membranes and blocking in 5% skimmed milk, we probed the membranes in TBS buffer containing 0.1% Tween 20 at 4°C overnight with diluted (1:5000) mouse anti-FlaA, anti-FliW2 polyclonal antibodies (in-house), or mouse anti-GroEL (Hsp60) monoclonal antibody (Product number H3524, Sigma-Aldrich, USA). GroEL served as an internal control.

2.8 | *In Silico* Predictions of FliW2, CsrA, and *flaA* RNA Secondary Structure

We used *H. pylori* J99 CsrA as a query to construct the phylogenetic tree analysis (Figure 1, left panel). The CsrA homologs (Table S3) from a range of representative taxa spanning proteobacteria were aligned using (standalone) MAFFT v7.526, the L-INS-i method, and default settings [34]. With the alignment as input, a distance matrix was generated using the WAG amino acid model implemented in phangorn v2.12.1 in R v4.4.1 [35]. A tree topology was generated via UPGMA (unweighted pair group method with an arithmetic mean) and also implemented in phangorn. Bootstrap analysis was carried out and the results

were plotted using phangorn's plotBS() function. Protein homolog comparison (Figure 1, right panel) was performed using the *H. pylori* J99 CsrA (UniProt ID: Q9ZJH4), FliW1 (UniProt ID: Q9ZK60), and FliW2 (UniProt ID: Q9ZJL5) as queries for protein identity analysis. The alignments were executed using Clustal O (version 1.2.4) on the UniProt website with default settings. The UniProt accession numbers for the CsrA homologs and FliW homologs are listed in Tables S3 and S4, respectively.

To compare the structure and conservation of *H. pylori* J99 FliW1 and FliW2 (Figure S2), we used MMseqs2 (version 71dd32ec43e3ac4dabf111bbc4b124f1c66a85f1) for a single-against-many search for homologous sequences using FliW1 (UniProt ID: Q9ZK60) and FliW2 (UniProt ID: Q9ZJL5) as query sequences. This strategy was implemented in ColabFold v1.5.5 [36], a structural prediction tool containing AlphaFold2 and hosted as a Jupyter Notebook (https://colab.research.google.com/github/sokrypton/ColabFold/blob/main/AlphaFold2.ipynb). ColabFold uses three databases: UniRef30 (a clustered version of UniRef100), PDB70 and a bespoke environmental dataset hosted by ColabFold (https://colabfold.mmseqs.com) in the homology search. The procedure employed limits the number of sequences in each multiple sequence alignment (MSA), reducing redundancy therein, while collecting sequences within (and retaining similar sequences between) buckets with different degrees of similarity to the query sequence, that is, it samples diverse sequences inferred by the query while reducing the overall alignment size. ColabFold was run with default parameters via the online notebook. For the MSA these parameters were "msa_mode=mmseq2_uniref_env and pair_mode=unpaired_paired."
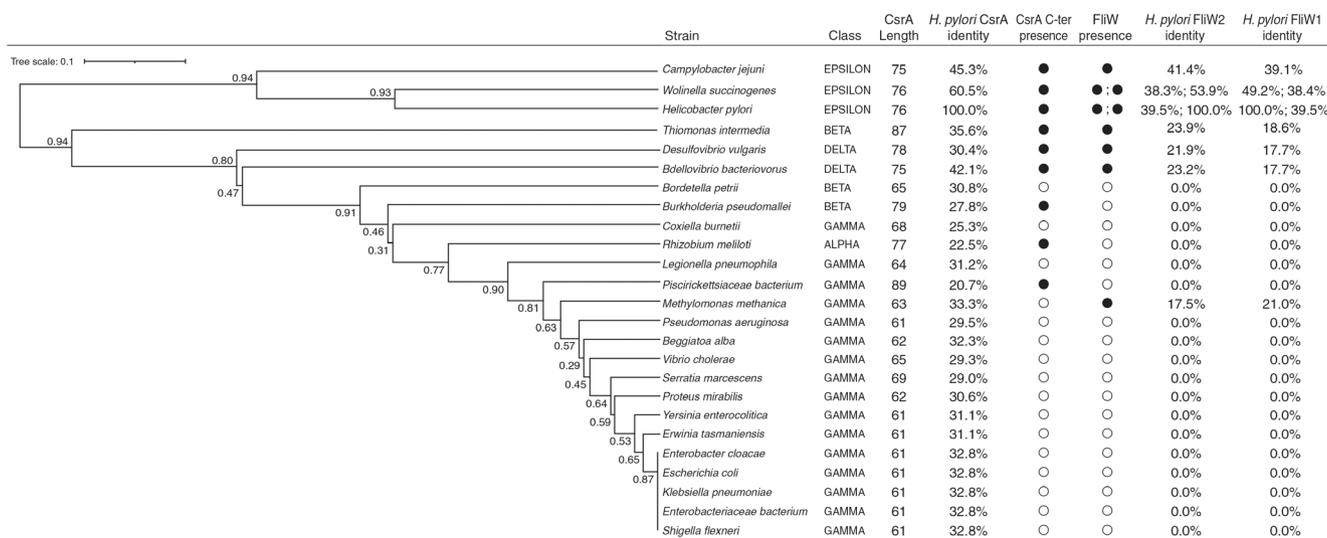
Strain	Class	CsrA Length	*H. pylori* CsrA identity	CsrA C-ter presence	FliW presence	*H. pylori* FliW2 identity	*H. pylori* FliW1 identity
Campylobacter jejuni	EPSILON	75	45.3%	●	●	41.4%	39.1%
Wolinella succinogenes	EPSILON	76	60.5%	●	● ; ●	38.3%; 53.9%	49.2%; 38.4%
Helicobacter pylori	EPSILON	76	100.0%	●	● ; ●	39.5%; 100.0%	100.0%; 39.5%
Thiomonas intermedia	BETA	87	35.6%	●	●	23.9%	18.6%
Desulfovibrio vulgaris	DELTA	78	30.4%	●	●	21.9%	17.7%
Bdellovibrio bacteriovorus	DELTA	75	42.1%	●	●	23.2%	17.7%
Bordetella petrii	BETA	65	30.8%	○	○	0.0%	0.0%
Burkholderia pseudomallei	BETA	79	27.8%	●	○	0.0%	0.0%
Coxiella burnetii	GAMMA	68	25.3%	○	○	0.0%	0.0%
Rhizobium meliloti	ALPHA	77	22.5%	●	○	0.0%	0.0%
Legionella pneumophila	GAMMA	64	31.2%	○	○	0.0%	0.0%
Piscirickettsiaceae bacterium	GAMMA	89	20.7%	●	○	0.0%	0.0%
Methylomonas methanica	GAMMA	63	33.3%	○	●	17.5%	21.0%
Pseudomonas aeruginosa	GAMMA	61	29.5%	○	○	0.0%	0.0%
Beggiatoa alba	GAMMA	62	32.3%	○	○	0.0%	0.0%
Vibrio cholerae	GAMMA	65	29.3%	○	○	0.0%	0.0%
Serratia marcescens	GAMMA	69	29.0%	○	○	0.0%	0.0%
Proteus mirabilis	GAMMA	62	30.6%	○	○	0.0%	0.0%
Yersinia enterocolitica	GAMMA	61	31.1%	○	○	0.0%	0.0%
Erwinia tasmaniensis	GAMMA	61	31.1%	○	○	0.0%	0.0%
Enterobacter cloacae	GAMMA	61	32.8%	○	○	0.0%	0.0%
Escherichia coli	GAMMA	61	32.8%	○	○	0.0%	0.0%
Klebsiella pneumoniae	GAMMA	61	32.8%	○	○	0.0%	0.0%
Enterobacteriaceae bacterium	GAMMA	61	32.8%	○	○	0.0%	0.0%
Shigella flexneri	GAMMA	61	32.8%	○	○	0.0%	0.0%

Tree scale: 0.1

FIGURE 1 | Phylogenetic tree analysis and characteristics of the CsrA and FliW homologs in Proteobacteria. The protein sequences of *H. pylori* J99 CsrA and its homologs (Table S3) were used to perform phylogenetic tree analysis from a range of representative taxa spanning proteobacteria (left panel) using (standalone) MAFFT v7.526, the L-INS-i method and default settings. With the alignment as input, a distance matrix was generated using the WAG amino acid model implemented in phangorn. A tree topology was generated via UPGMA (unweighted pair group method with an arithmetic mean) and also implemented in phangorn. Bootstrap analysis was carried out and the results were plotted using phangorn's plotBS() function. In the right panel, further detail regarding the CsrA and FliW homologs is shown. Not all clades of Proteobacteria possess the carboxylterminal extension of CsrA or show the presence of FliW. Protein homolog comparison was performed using the *H. pylori* J99 proteins CsrA (UniProt ID: Q9ZJH4), FliW1 (UniProt ID: Q9ZK60), and FliW2 (UniProt ID: Q9ZJL5) as queries for protein identity analysis. It is of note that *H. pylori* J99 (the third species from the top) possesses the CsrA with the C-terminal extension and two FliW homologs. The identity of the *H. pylori* FliW1 is 39.5%, compared to the query, *H. pylori* FliW2 (100%).

Protein sequence alignment of the *H. pylori* J99 CsrA (UniProt ID: Q9ZJH4), FliW1 (UniProt ID: Q9ZK60), and FliW2 (UniProt ID: Q9ZJL5) homologs were carried out using CLC Genomic Workbench (version 24.0.1). The 3D structure of FliW2-CsrA interacting regions was predicted using ColabFold based on DeepMind AlphaFold2 [36] and reconstructed using PyMoL. The RNA secondary structure of the 5'UTR of *flaA* mRNA (50 bases) was executed in the RNA Folding Form V2.3 at the UNAFold Web Server (http://www.unafold.org/) with a default setting.

2.9 | In Vitro Pull-Down Assays

2.9.1 | *H. pylori* Experiment

To demonstrate that FliW2 interacts with CsrA in *H. pylori*, we first over-expressed recombinant C-terminal histidine-tagged CsrA protein (CsrA$_{His}$) from pET22b-*CsrA* (Table S1) in *E. coli* BL21(DE3) host cells. After sonication, we applied the *E. coli* lysate containing His-tagged CsrA proteins and protease inhibitors to the nickel-charged (Ni^{2+}) magnetic beads in Lysis Equilibration (LE) Buffer (50 mM phosphate buffer, 300 mM NaCl, 0.05% Tween 20, and 1.5 mg/mL Lysozyme; pH 8.0) at 4°C for overnight. This generated CsrA$_{His}$-bound Ni^{2+}-magnetic beads (CsrA-beads), which were washed twice in Wash Buffer (50 mM phosphate buffer, 300 mM NaCl, 10 mM imidazole; pH 8.0) and ready for protein–protein interaction. To prepare *H. pylori* lysates, 10 mL of freshly grown *H. pylori* cells were collected when they reached early stationary phase (OD$_{600}$ = 4–6). The *H. pylori* cells were washed and resuspended in ice-cold LE Buffer containing lysozyme, DNase I, RNase A, and protease inhibitors, followed by sonication. After centrifugation at 2000×*g* for 15 min at 4°C to remove cell debris, the supernatants of *H. pylori* lysates were saved and ready for protein pulldown assay. We then pooled the CsrA$_{His}$-bound beads with the lysates of *H. pylori* WT or Δ*fliW2* as prey proteins and mixed using an inverter at 4°C for 2 h. After washing, we added 100 μL Elution Buffer (50 mM phosphate buffer, 300 mM NaCl, 500 mM imidazole; pH 8.0) to elute CsrA$_{His}$ and its interacting proteins. The eluents were examined using Western blotting. FlaA and FliW2 were probed using mouse anti-FlaA and anti-FliW2 polyclonal antibodies, respectively. The negative control group was the *H. pylori* Δ*fliW2* lysate pooled with CsrA$_{His}$.

2.9.2 | *E. coli* Experiment

We over-expressed CsrA$_{His}$ (pET22b-CsrA) and tag-free FliW2 (pET22b-FliW2-noHis) (Table S1) in *E. coli* BL21 (DE3) cells, respectively, by induction using isopropyl-β-D-thiogalactopyranoside (IPTG) at 0.4–0.6 ODU. The *E. coli* cells were incubated at 25°C for 4 h, harvested by centrifugation at 9020*g* for 20 min, and resuspended in Binding Buffer (20 mM HEPES, 500 mM NaCl, 10% glycerol, 1 mM β-mercaptoethanol, pH 7.5). We pooled 3 L of *E. coli* (pET22b-FliW2-noHis) and 1 L of *E. coli* (pET22b-CsrA) cells, and underwent bacterial disruption by sonication. The resulting supernatant was loaded onto a nickel-NTA affinity column (Ni Sepharos 6 Fast Flow, GE Healthcare) **t**hat was previously equilibrated in Binding Buffer. The column was sequentially washed in Buffer A (20 mM HEPES, 300 mM NaCl, 1 mM β-mercaptoethanol, pH 7.5) containing 25 mM imidazole. Proteins were eluted in Buffer A supplemented with 300 mM imidazole. The eluted proteins were examined by SDS-PAGE, followed by Coomassie brilliant blue staining and analysis.

2.10 | Bacterial Two-Hybrid Analysis

We chose an in vivo approach, the Bacterial Adenylate Cyclase-based Two-Hybrid (BACTH) system (Euromedex, France), to examine the interaction between CsrA and FliW2. In brief, pKT25 (N-terminal T25 segment fusion) serves as a vector for constructing a bait protein, while pUT18 (C-terminal T18 segment fusion) vector is used for a target protein. The *fliW2* gene and *csrA* gene carrying various deletions were individually PCR-amplified, *Bam*HI/*Acc*65I-digested, and cloned into the *Bam*HI/*Acc*65I-cleaved pKT25 and pUT18 vectors (Table S1). After Sanger sequencing validation on the constructed clones, pKT25- and pUT18-derivative clones were co-transformed into an *E. coli* reporter strain DHM1. The transformants were grown in LB broth with ampicillin, kanamycin, and IPTG for 16 h, then the cells were lysed and extracted for β-galactosidase activity measurement. An increase of β-galactosidase activity in Miller units is an indication of positive protein–protein interactions. *E. coli* DHM1 cells harboring vectors pKT25 and pUT18 served as a negative control, whereas the cells harboring pKT25-FeoB and pUT18-FeoC were a positive control [37]. We also included background signal controls to distinguish false-positive protein interactions.

2.11 | Ethics Statement

Animal experiments were reviewed and approved by the Institutional Animal Care and Use Committee of National Cheng Kung University, Taiwan (approval number: 109127). Animal well-being, sedation, and analgesia were monitored and administered as indicated to minimize stress and pain associated with any veterinary procedures.

2.12 | Statistical Analysis

Statistical analysis was assessed using an unpaired *t* test with Welch's correction, one-way or two-way analysis of variance (ANOVA) (GraphPad Prism 8). Statistical significance was represented as *, $p < 0.05$; **, $p < 0.01$; ***, $p < 0.001$; and ****, $p < 0.0001$ unless indicated.

3 | Results

3.1 | Evolutionary Characteristics of the CsrA and FliW2 Homologs in *H. pylori* and Proteobacteria

We identified two *fliW* homologs (*jhp1081*-encoded FliW1 and *jhp1291*-encoded FliW2) from the *H. pylori* J99 genome using the BLAST analysis. Subsequently, we constructed multiple sequence alignments (MSAs) using MMseqs2 for comparison against diverse sequences (Figure S2). Our result showed a more consistent sequence coverage distribution across the length of FliW2 than across the length of FliW1, particularly among the bulk of the sequences that have intermediate similarities to the query. It appears

that the N-terminal region of FliW1 is less well-represented in MSAs than that of FliW2. This analysis implied that the *H. pylori* FliW2 is more likely to be conserved than the FliW1. Our proteome analysis of the *H. pylori* J99 wild-type strain also showed that FliW2 production was ten-fold more than that of FliW1 in neutral or acidic media (Table S5). Further phylogenetic tree analysis was carried out to investigate whether *H. pylori* CsrA has an association with the FliW2 protein over macroevolutionary time scales. We identified the presence of *csrA* and *fliW* genes and extracted their protein sequences from the genomes of the representative members of Proteobacteria. Interestingly, *H. pylori*'s CsrA sequence is approximately 15 residues longer at the carboxyl terminus than that of Gammaproteobacteria (Figure 1, right panel). Based on evidence presented elsewhere in this paper, *H. pylori* CsrA likely interacts with FliW2. As well, we found that most Gammaproteobacteria do not contain FliW proteins (Figure 1, right panel). Therefore, the genomic characteristics of these CsrA and FliW2 show that *H. pylori* differs from other Proteobacteria (Figure 1, left panel). We also predicted the RNA secondary structure of the 5′ un-translational region (UTR) of the major flagellin *flaA* transcript, revealing two hairpin structures containing the CsrA binding motif NGGA (Figure S3). This finding was in agreement with the hypothesis that CsrA dimers bind to the *flaA* mRNAs in *C. jejuni* [14]. We therefore hypothesized that FliW2 modulates CsrA by allosteric obstruction of target transcripts (i.e., the major flagellin *flaA*), thus de-repressing the motility of *H. pylori*.

3.2 | Disruption of *fliW2* Impairs the Flagellar Motility of *H. pylori*

To discover the function of FliW2, we constructed an in-frame deletion mutant of *fliW2* using a gene replacement approach. The resultant Δ*fliW2* mutant was validated using Sanger sequencing and cDNA-qPCR analysis, confirming that the Δ*fliW2* mutant had no polar effects (Figure S1). We examined the motility of the Δ*fliW2* mutant in the soft agar plates. Our results showed that, unlike the WT cells, the Δ*fliW2* mutant cells lost motility in both the neutral and acidic media (pH 7 and 6), similar to the non-motile Δ*flaA* cells (Figure 2A). We also studied the flagellar structure of the Δ*fliW2* mutant cells using scanning electron microscopy. The Δ*fliW2* mutant cells were primarily aflagellate or had only short-protruding flagella, differing from the long tangled flagellar filaments observed in the WT cells (Figure 2B). To further investigate the non-motile Δ*fliW2* mutant cells, we analyzed the expression of the major flagellin FlaA by Western blotting. The FlaA expression was substantially reduced in the Δ*fliW2* mutant cells (Figure 2C), indicating that FliW2 modulates FlaA expression through direct or indirect regulations. In order to test our hypothesis, we investigated whether or not FliW2 interacts with CsrA.

3.3 | Interaction Between FliW2 and CsrA Proteins

To demonstrate protein interactions between FliW2 and CsrA, we carried out pull-down assays. We generated nickel ion magnetic beads bound with recombinant histidine-tagged CsrA protein (CsrA$_{His}$). By applying the total lysate of the *H. pylori* WT strain to the beads, it allowed us to detect the proteins that
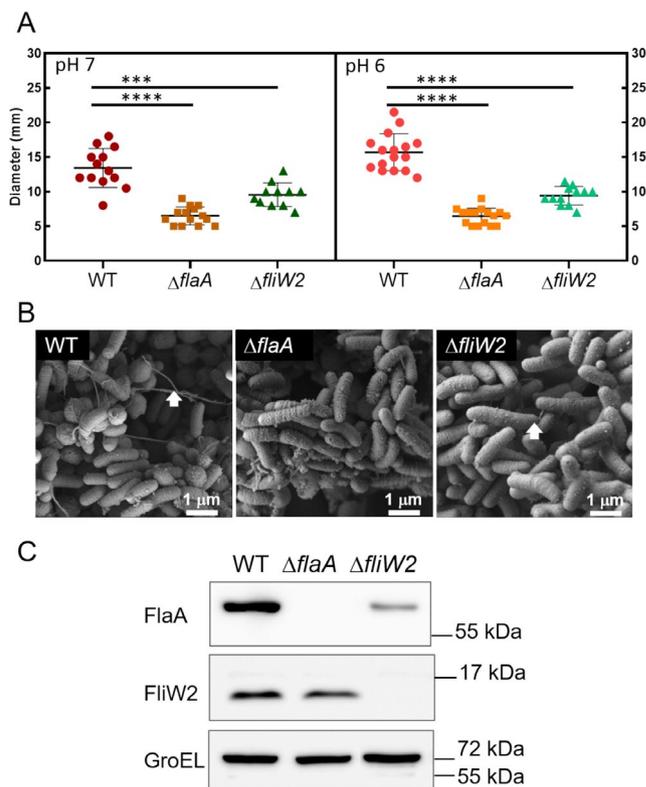

FIGURE 2 | Examination of the motility and flagellation of *H. pylori* Δ*fliW2* strain. (A) Swarming motility examination. *H. pylori* wild-type (WT, circle symbol), the non-motile Δ*flaA* mutant (square symbol), and the Δ*fliW2* mutant (triangle symbol) strains were inoculated on the Brucella soft agar plates at pH 7 (left plot) and pH 6 (right plot). The diameter of bacterial motility was recorded and calculated as the mean ± SD of at least three biological replicates. Error bars are standard deviation. An unpaired *t* test with Welch's correction was applied to calculate the statistical significance (***p < 0.0005; ****p < 0.0001). (B) Scanning electron microscopic analysis on bacterial morphology and flagellation. Bacterial morphology and flagellar structure were examined in the WT (left plot), Δ*flaA* (middle plot), and Δ*fliW2* (right plot) strains after 55–60 h of inoculation. The formed flagellar filaments are indicated (white arrows). The non-motile Δ*flaA* mutant cells were mostly aflagellate, though some possessed short flagella. The micrographs were taken from three fields in two independent experiments. Scale bars represent 1 μm. (C) Expression of major flagellin FlaA by Western blot analysis. Western blot analysis was carried out to examine the expression of FlaA extracted from the whole-cell proteins of the WT, Δ*flaA*, and Δ*fliW2* strains at the early stationary phase. FlaA and FliW2 were probed using mouse polyclonal antibodies, while a mouse monoclonal antibody was used to detect GroEL. GroEL served as an internal control. The absence of the FlaA and FliW2 signals showed the specificity of anti-FlaA and anti-FliW2, respectively.

interact with CsrA$_{His}$ under native conditions. After washing, the FliW2 signal was revealed in the eluted fraction by Western blotting (Figure 3A, Lane 7). To determine whether or not FliW2 binds to CsrA directly, we overexpressed the recombinant CsrA$_{His}$ (pET22b-CsrA) (Figure 3B, Lane 3) and the recombinant tag-free FliW2 (pET22b-FliW2-noHis) (Figure 3B, Lane 5), respectively, in *E. coli* BL21 (DE3) cells. Then we pooled the *E. coli* lysate containing FliW2 proteins with the other *E. coli* lysate, which contained CsrA$_{His}$ proteins. As we hypothesized, the
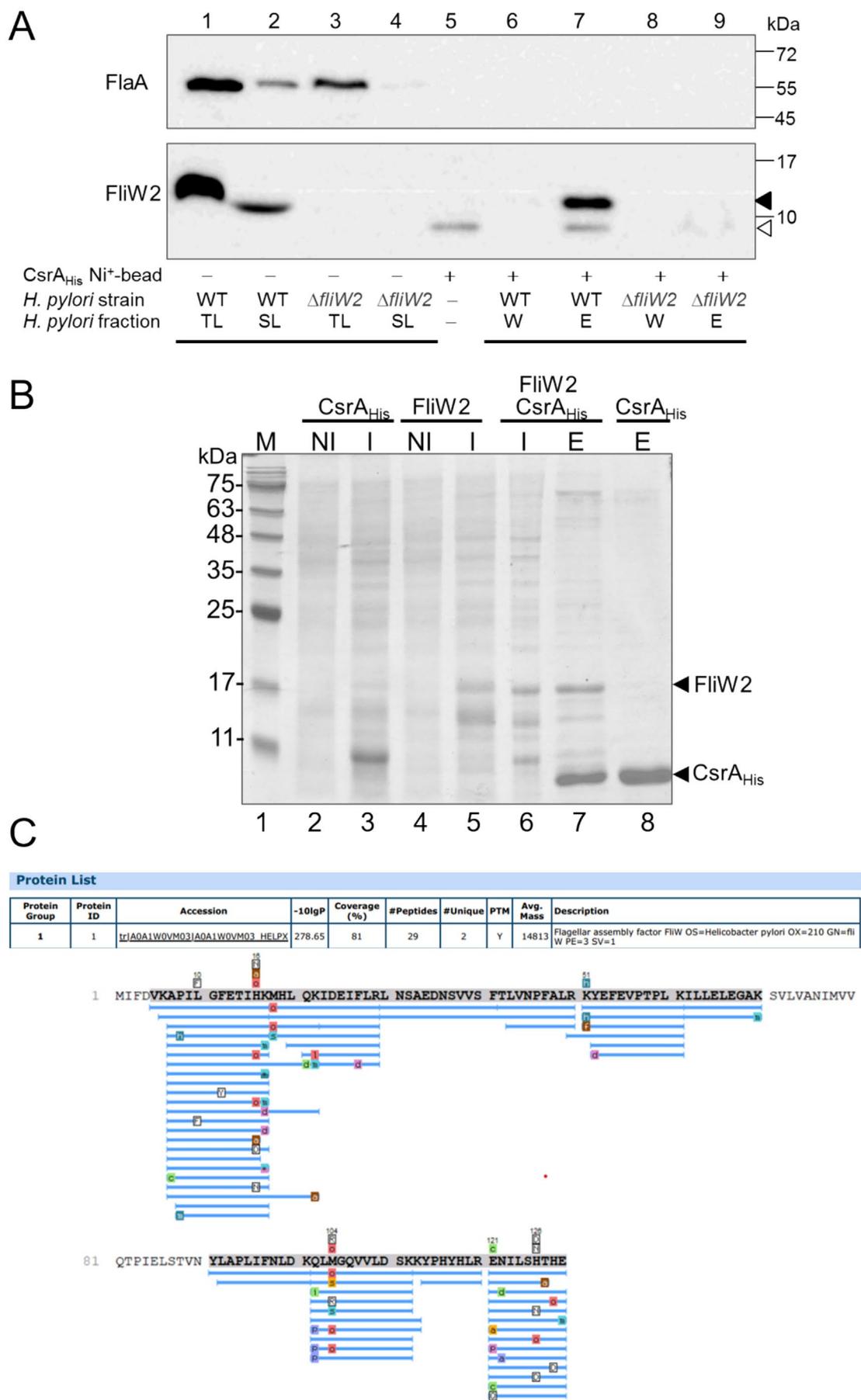
FIGURE 3 | Legend on next page.

FIGURE 3 | Investigation on CsrA-FliW2 interaction by pull-down assays and liquid chromatography with tandem mass spectrometry (LC–MS/MS) analysis. (A) Pull-down assay using *H. pylori* lysates. The recombinant polyhistidine-tagged CsrA protein (CsrA$_{His}$) was overexpressed in the *E. coli* BL21(DE3) host cells, captured, and purified by nickel-charged magnetic beads under a native condition. Once the CsrA$_{His}$-bound Ni$^+$-magnetic beads were prepared, we applied the sonication lysate (SL) from the *H. pylori* wild-type (WT) cells or the Δ*fliW2* cells. After a series of wash steps, the proteins that bound to CsrA$_{His}$ were co-eluted and analyzed using Western blotting. The presence of FliW2 signals (~15 kDa, solid triangle) in the eluent of the *H. pylori* WT lysate and CsrA$_{His}$-bound beads (lane 7) indicated that CsrA interacted with FliW2. The open triangle indicates the non-specific signal of anti-FliW2 antibody. In addition to this, in the control group where the *H. pylori* Δ*fliW2* lysate was pooled with CsrA$_{His}$, the absence of FliW2 signals (lane 9) confirmed the FliW2-CsrA$_{His}$ interaction. Detection of the FlaA protein served as internal control. The data shown was the representative of three independent experiments. TL stands for total lysate, SL for sonication lysate, W for wash fraction, and E for elution fraction. (B) Pull-down assay using hetero-expression in the background of *E. coli* cells. We overexpressed the recombinant CsrA$_{His}$ (pET22b-CsrA) (lane 3) and the recombinant tag-free FliW2 (pET22b-FliW2-noHis) (lane 5), respectively, in the *E. coli* BL21(DE3) host cells. After IPTG induction, the *E. coli* cell lysates were prepared by sonication and pooled. After pooling, the resulting supernatant was loaded onto a nickel-NTA affinity column, washed, and the proteins that bound to the nickel column and CsrA$_{His}$ were eluted. The eluted proteins were examined by SDS-PAGE and stained. We found the abundant protein bands (15 kDa and 9 kDa) that were presumably tag-free FliW2 proteins and CsrA$_{His}$ (lane 7). The data shown was the representative of two biological replicates. M stands for protein marker, NI for non-induction, I for induction, and E for elution fraction. (C) The validation of CsrA-bound FliW2 protein by LC–MS/MS analysis. The overexpressed protein band (15 kDa) from Figure 3B (lane 7) was excised and underwent in-gel trypsin digestion for protein identification using LC–MS/MS analysis. The peptide fragments that matched to those of the FliW2 protein of *H. pylori* J99 are highlighted in gray in the figure.

---

tag-free FliW2 was co-eluted with the CsrA$_{His}$ through nickel column separation, showing that the FliW2 directly interacted with the CsrA (Figure 3B, Lane 7). The overexpressed protein band (~15 kDa) was then excised, purified, and analyzed by liquid chromatography with tandem mass spectrometry. The matched peptide fragments of *H. pylori* FliW2 were identified (Figure 3C). The combined results of these investigations demonstrate that *H. pylori* FliW2 interacts directly with CsrA.

3.4 | AlphaFold2 Prediction of FliW2-CsrA Interacting Regions

To identify the FliW2-CsrA interacting regions, we took advantage of the deep learning algorithm AlphaFold2 (AF2) to predict the pattern of protein interactions. As shown in Figure 4A (Left panel), the β-barrel region of FliW2 formed a cleft that is predicted to interact with CsrA. The structure of *H. pylori* CsrA contains the N-terminal β-strands region and a loop–helix–loop–helix region, where we predicted that the C-terminal extension helix–loop–helix (residues 55–76) would interact with FliW2 (Figure 4A, right panel). The findings of earlier loss-of-function studies of the FliW and CsrA in *B. subtilis* and *C. jejuni* [38, 39] allowed us to postulate the crucial residues of FliW2 (F27, Q106, and V108) and CsrA's core proximal cluster (N55) for protein binding (Figure 4B,C). Subsequently, we designed successive truncations of CsrA to determine the region that is essential for the CsrA-FliW2 binding based on our predictions. The deletion of the C-terminal extended helix–helix structure of CsrA occurs in CsrA$_{1-72}$ (4-residue deletion), CsrA$_{1-63}$ (13-residue deletion), CsrA$_{1-58}$ (18-residue deletion), and CsrA$_{1-54}$ (22-residue deletion) (Figure 4A, right panel).

3.5 | Determination of the Critical Regions of CsrA for FliW2 Interaction In Vivo

Following our AF2 prediction, we performed in vivo bacterial two-hybrid analysis to determine FliW2-CsrA interactions and the regions required for the FliW2-CsrA binding. We chose the Bacterial Adenylate Cyclase-based Two-Hybrid (BACTH) system to generate T25-fused bait proteins using pKT25 (N-terminal T25 fusion) and T18-fused target proteins using pUT18 (C-terminal T18 fusion). In our first set of experiments, we detected the activity of β-galactosidase by analyzing T25-fused FliW2 and T18-fused CsrA, and T18-fused CsrA truncating proteins (Figure 5, upper panel). The increase in β-galactosidase activity observed in samples 3, 5, and 7 showed that FliW2 was bound to full length CsrA, CsrA$_{1-72}$, and CsrA$_{1-63}$. With the elimination of the C-terminus end 18 and 22 residues of CsrA, FliW2 could not bind to CsrA$_{1-58}$ or CsrA$_{1-54}$ and the β-galactosidase activity was not significantly elevated compared to negative controls (Samples 9 and 11). To verify whether the C-terminal extension of CsrA for FliW2 binding was not an artificial defect, we created T25-fused CsrA proteins (full-length or with truncations) and T18-fused FliW2 in our second set of experiments (Figure 5, lower panel). Consistently, the binding between CsrA and FliW2 was absent when the C-terminal 18 and 22 residues of CsrA were deleted (Samples 20 and 22). Taken together, these results showed that the C-terminal region of CsrA is crucial for interaction with FliW2.

4 | Discussion

In this study we have characterized the *H. pylori* flagellar assembly factor FliW2 that interacts directly with the posttranscriptional global regulator CsrA. Hence, FliW2 may affect CsrA's repression of the major flagellin FlaA expression and flagellar biosynthesis (Figure 6). Based on our *in silico* analyses, we postulated that the *H. pylori* FliW2 protein modulates CsrA functionality based on (i) CsrA binding motifs predicted at the 5′-UTR of the *flaA* mRNA; (ii) the region of CsrA for binding to FliW homologs; and (iii) the identification of *fliW* homologs, *fliW1* and *fliW2*, in the genome of *H. pylori*. The phenotypic analyses of the isogenic Δ*fliW2* mutant cells clearly demonstrated that the loss of FliW2 diminishes *H. pylori*'s flagellar formation and motility, as well as the production of FlaA. Further prediction of the
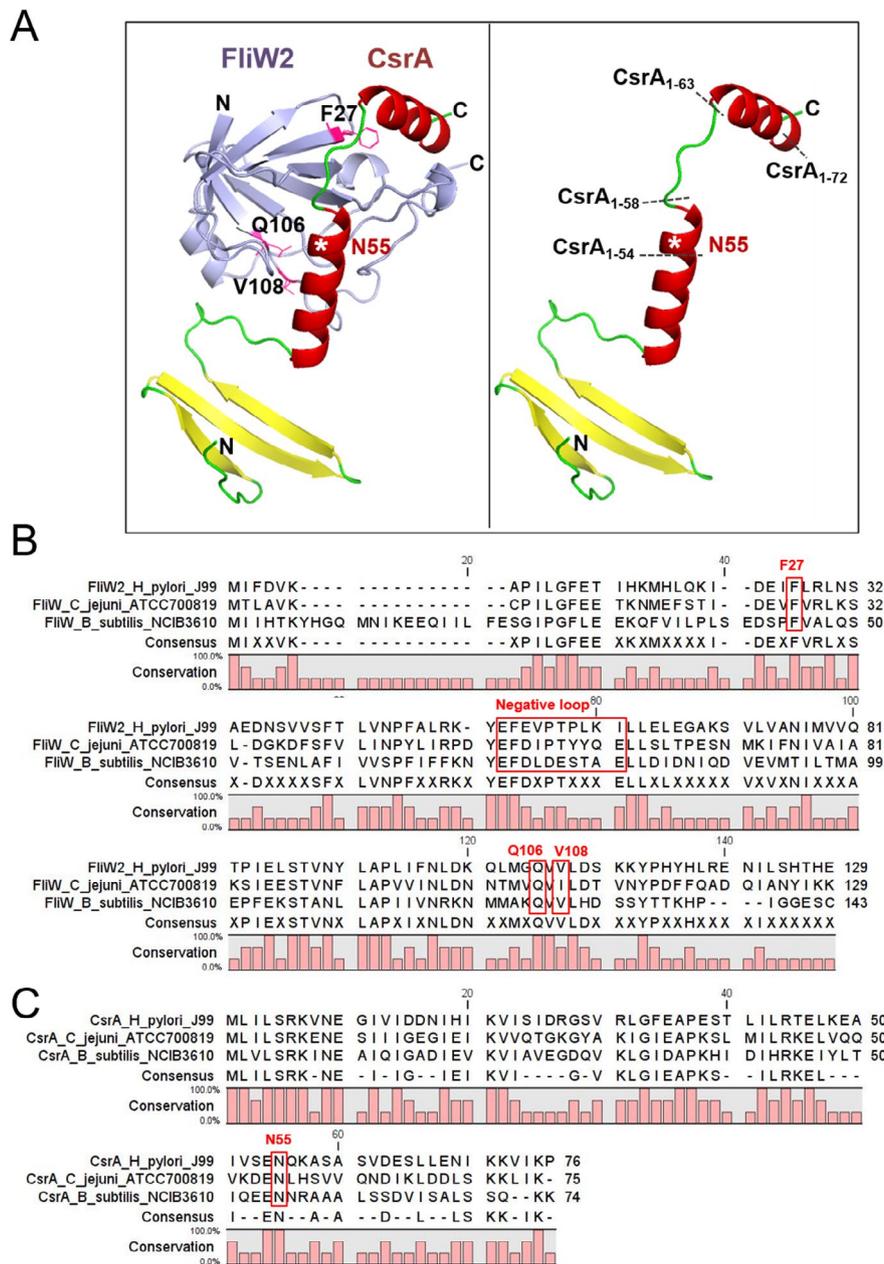
FIGURE 4 | *In silico* prediction of the FliW2 and CsrA proteins. (A) AlphaFold2 prediction of CsrA-FliW2 interaction. The three-dimensional structure of the FliW2-CsrA complex was predicted using AlphaFold2. The FliW2 protein consists of the β-sheet regions (left plot, colored lavender), where the previously reported conserved residues for CsrA binding are indicated [38]. CsrA (full length, 1–76 residues) contains the N-terminal β-sheet region and a loop–helix–loop–helix region. It should be noted that the C-terminal extension of CsrA that forms the loop–helix structure might be crucial for FliW2 binding. Therefore, we designed several C-terminal truncations: CsrA$_{1-72}$ (4-residue deletion), CsrA$_{1-63}$ (13-residue deletion), CsrA$_{1-58}$ (18-residue deletion), and CsrA$_{1-54}$ (22-residue deletion). (B) Protein sequence alignment of the FliW2 homologs. The FliW2 (UniProt ID: Q9ZJL5) of *H. pylori* strain J99/ATCC 700824, the FliW (UniProt ID: Q0P9H9) of *C. jejuni* strain ATCC 700819/NCTC 11168, and the FliW (UniProt ID: A0AAE3WUD6) of *B. subtilis* strain NCIB 3610/ ATCC 6051 were aligned and analyzed. The negative loop and the location of the residues (F27, Q106, V108) that were reported conserved for FliW2 binding to CsrA are labeled. (C) Protein sequence alignment of the CsrA homologs. The CsrA (UniProt ID: Q9ZJH4) of *H. pylori* strain J99/ATCC 700824, the CsrA (UniProt ID: Q0P9F1) of *C. jejuni* strain ATCC 700819/NCTC 11168, and the CsrA (UniProt ID: A0AAE3WX71) of *B. subtilis* strain NCIB 3610/ ATCC 6051 were aligned and analyzed. The location of the conserved active site N55 for CsrA to bind FliW2 is labeled.

CsrA-FliW2 interactive domains by the AlphaFold2 algorithm revealed the crucial binding regions that were then examined using in vitro pull-down assays and in vivo bacterial two-hybrid system analysis. Our data points to novel regulatory roles that the *H. pylori* flagellar assembly factor FliW2 has in obstructing CsrA activity and in antagonizing CsrA's regulation of *flaA* mRNA processing and translation. This may have implications for the control of flagellar motility in *H. pylori*.
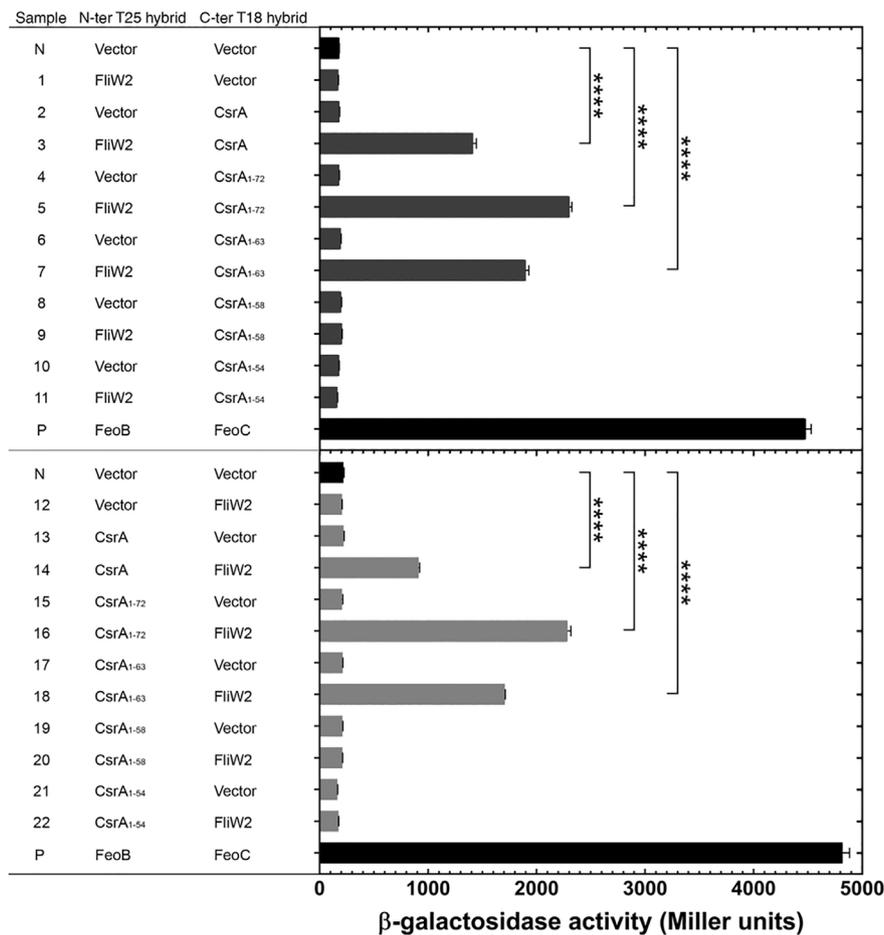
FIGURE 5 | Validation of in vivo CsrA-FliW2 interaction using a bacterial two-hybrid system. The Bacterial Adenylate Cyclase-based Two-Hybrid (BACTH) system was employed to detect protein interactions by measuring the activity of β-galactosidase in the *E. coli* DHM1 strain. In brief, in the first experimental set (upper panel), the *fliW2* gene was cloned into pKT25 (N-terminal T25 fragment fusion; bait vector) to form T25-FliW2. The full-length or truncated *csrA* gene was cloned into pUT18 (C-terminal T18 fragment fusion; target vector) to form T18-CsrA. The pKT25- and pUT18-derived plasmids were co-transformed into the *E. coli* DHM1 strain. After inoculation with IPTG for 16 h, the cells were extracted for the measurement of their β-galactosidase activity. In the second experimental set (lower panel), we instead created T25-CsrA including truncated forms and T18-FliW2 to examine their protein interactions. An increase of measured β-galactosidase activity in Miller units is an indication of positive interaction. *E. coli* DHM1 cells harboring pKT25 and pUT18 served as negative controls and those harboring pKT25-FeoB and pUT18-FeoC served as positive controls. The background signal controls (vectors) were included to identify false-positive interactions. The data shown was the representatives of three biological replicates and calculated as mean ± SD. Error bars are standard deviation (**** $p < 0.0001$).

The biogenesis of flagella in *H. pylori* and *C. jejuni* is tightly regulated by regulators and small RNAs, and significantly different from that in the Gammaproteobacteria *E. coli* due to the lack of the master regulator FlhDC. Interestingly, König et al. recently discovered novel posttranscriptional non-coding small RNAs, the RpoN-dependent CJnc230 and the FliA-dependent CJnc170, that fine tune the hierarchical regulation of flagellar biogenesis in *C. jejuni* [8]. In contrast to this finding, small RNA-mediated posttranscriptional regulation in stress response and virulence control has been reported in *H. pylori* [11, 40–42]. The *cag*-PAI encoded small RNA CncR1 down-regulates a flagellar checkpoint factor *fliK* and promotes the expression of *H. pylori* adhesins [11]. As well, the small RNA RepG (regulator of polymeric G-repeats) found in *H. pylori* not only controls lipopolysaccharide phase variation but also the variable G-repeat in the mRNA leader of a chemotaxis receptor gene *tlpB* [40]. However, there has been no small RNA study reported in relation to the

modulation of CsrA in *H. pylori* or *C. jejuni*. Even though we could not rule out the possibility of small RNAs regulating CsrA, our study evidently supports the possibility of an alternative mechanism in which FliW2 indirectly modulates flagellar genes posttranscriptionally via protein allosteric antagonism on riboregulator CsrA.

We also give an explanation for the biological meaning of FliW1 and FliW2 in the *H. pylori* of Epsilonproteobacteria. Since the genome of *H. pylori* is merely 1.6 M base-pairs in length and the co-occurrence of *fliW* paralog is widespread (Figure 1), it seems unusual that it possesses two *fliW* homologous genes in *H. pylori*. We postulated that *H. pylori* requires FliW1 and FliW2 to antagonize CsrA repression of flagellar biogenesis for *H. pylori*'s survival in the human gastric niche under heterogeneous conditions. Previous studies have reported that flagellar and chemotactic motility remarkably increases the survival of
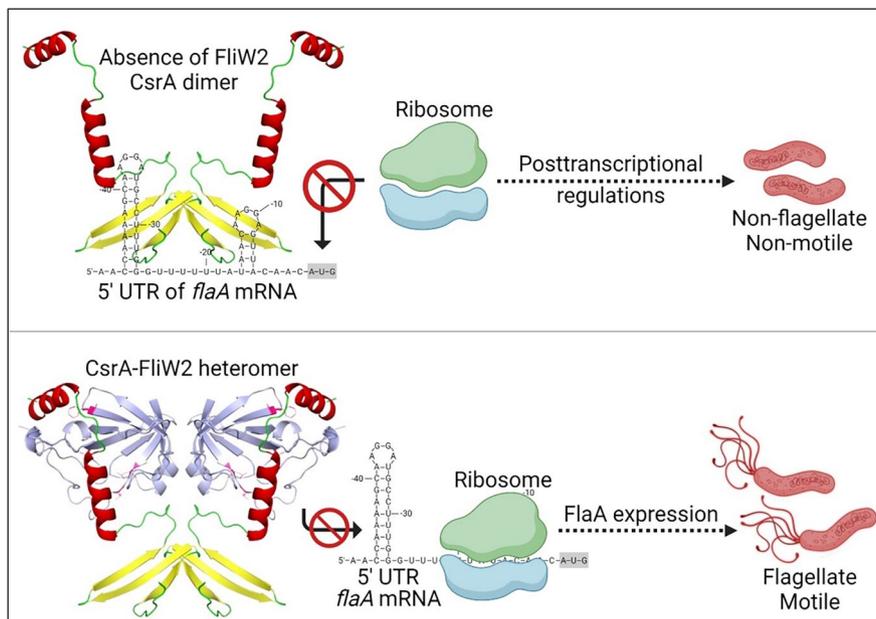
FIGURE 6 | A model of the allosteric obstruction of FliW2 to CsrA that attenuates the effect of CsrA on the motility of *H. pylori*. In the absence of FliW2 (upper panel), CsrA proteins are free to form dimers. The CsrA dimers bind to either a target transcript itself or its 5′ un-translational region (UTR), where CsrA motifs (NGGA) are overlapped with ribosomal binding sites (RBSs). Since the RBSs are blocked, ribosomes are unable to initiate the translation of the target transcripts (i.e., major flagellin *flaA*) and may affect the processing of the target transcripts. This then reduces the expression of FlaA and FlaA-associated flagellar formation. As a consequence, CsrA modulates the motility of *H. pylori* through a negative regulatory mechanism at the posttranscriptional level. However, when FliW2 is present (lower panel), FliW2 interacts with CsrA to form heterodimers, thus FliW2 obstructs CsrA by binding to allosteric sites of CsrA at its C-terminal extension, differing from the RNA binding regions. Therefore, the conformational structures of FliW-CsrA heterodimers preclude binding to the target transcripts. This allows ribosomes to bind and start the translation of the mRNAs, attenuating the negative regulation of CsrA. Taken together, FliW2 de-represses the motility of *H. pylori* by the allosteric obstruction of CsrA.

H. pylori in the extremely acidic environment of the stomach by allowing the bacteria to rapidly swim and colonize the mucin layer of the gastric epithelium [6, 12]. Therefore, despite the known regulatory cascade of flagellar biosynthesis in *H. pylori*, CsrA aids in governing the expression and assembly of flagellar filaments [18, 43]. This implies the importance of *H. pylori* utilizing FliW1 and FliW2 to antagonize CsrA repression in different ways. The supporting data includes our genomic analyses (Figure 1 and Figure S2) showing that the *fliW2* gene is likely more conserved than the *fliW1* gene, and our proteome analysis of *H. pylori* J99 indicates that the expression of FliW2 is approximately ten-fold higher than FliW1 (Table S5). This could explain our observation on the short flagellar filament and trace amount of FlaA production in the Δ*fliW2* mutant (Figure 2B,C), possibly due to the positive FliW1-CsrA interaction in the bacterial two-hybrid assay (data not shown). Nonetheless, Niehus et al. propose a transcriptional regulation model in the flagellar system in several *H. pylori* strains. In their model, the *fliW1* (HP1154) gene belongs to the middle stage (class 2) flagellar genes whose expression is modulated by the alternative sigma factor RpoN54 and FlgR regulator. On the other hand, the expression of the *fliW2* (HP1377) gene is presumably under the control of the housekeeping RpoD [7]. It seems possible that *H. pylori* FliW1 and FliW2 modulate CsrA at the different stages of flagellar biosynthesis, though there has been no evidence demonstrating that *fliW1* and *fliW2* are differentially regulated. This mechanism is not yet understood and remains to be explained. Additionally, investigating the

Δ*fliW1* knockout and/or the Δ*fliW1*Δ*fliW2* double knockout strains of *H. pylori* would significantly improve our understanding of whether *fliW1* also plays a role in the antagonism of CsrA and in the FlaA regulation. More interestingly, the key residues of *H. pylori* FliW1-FliW2-CsrA interaction are worthy of further investigation to distinguish the physiological roles in the FliW1-CsrA and the FliW2-CsrA. Discovering how the FliW1-FliW2-CsrA interaction alters the modulation of *flaA* mRNA would require delicate investigations such as protein–protein and protein-RNA crystal structures to find the key conformations and residues of the FliW1-FliW2-CsrA-*flaA* mRNA complex. Collectively, our findings support the hypothesis that FliW2 is the dominant antagonist of CsrA and de-represses *H. pylori*'s motility.

The truncations on the C-terminal extension of *H. pylori* CsrA demonstrate the importance of its interaction with the FliW2 protein. Our in vivo bacterial hybrid-system showed the residues 59–63 of CsrA (Figure 5), which was predicted to be a loop structure (Figure 4A), might have an uncovered significant role in binding to FliW2. Nonetheless, the truncated CsrA proteins may be unstable as they have not been tested. Another interesting finding is that the residues constituting the negative loop of *H. pylori* FliW2 obtains only two negatively charged residues (E53 and E55) (Figure 4B), compared to that of *B. subtilis* FliW (E71, D73, D75, E76, and E80) [38]. This suggests that the negative loop of the *H. pylori* FliW2 might not cause a strong electrostatic repulsion with the SD sequence like the *B. subtilis*

FliW does to hinder RNA interaction. Hence, the *H. pylori* flagellar biosynthesis system would serve as an interesting model to study the co-evolution between the loss of CsrA's C-terminal extension in association with FliW1, FliW2, and small RNAs (CsrB/D) in proteobacteria. The outcome would help us to understand why in Gammaproteobacteria the CsrA proteins without the C-terminal extension are modulated by small RNAs but not FliW antagonism.

In conclusion, we propose a model of the allosteric obstruction of FliW2 to CsrA that de-represses the motility of *H. pylori* (Figure 6). In the absence of FliW2, CsrA proteins form homodimers binding to the overlapping CsrA motif-ribosomal binding sites of a target transcript. This may affect the translation of the target transcripts and/or their mRNA processing, thus influencing the expression of FlaA and flagellar formation. As a consequence, CsrA modulates the motility of *H. pylori* through a negative regulatory mechanism at the posttranscriptional level. However, when FliW2 is present, it interacts with CsrA to form heterodimers. The conformation of the FliW2-CsrA heterodimers prevents them from binding to the target transcripts. This allows ribosomes to bind and start the translation of the target transcripts, attenuating the negative regulation of CsrA. Taken together, FliW2 de-represses the flagellar motility of *H. pylori* by the allosteric obstruction of CsrA.

Author Contributions

M.S.-W.S. conceptualized research; M.S.-W.S., B.D., F.Y.K., W.-J.T., Y.-L.C., J.-W.C., S.W., and P.-J.T. performed research; M.S.-W.S. and B.D. wrote and edited the manuscript. J.-J.W. supervised the project, edited the manuscript, and obtained research funding. All authors read and approved the final manuscript.

Ethics Statement

The authors have nothing to report.

Consent

The authors have nothing to report.

Conflicts of Interest

The authors declare no conflicts of interest.

Data Availability Statement

The dataset supporting the conclusions of this article is included in the article.

References

1. C. Lei, Y. Xu, S. Zhang, C. Huang, and J. Qin, "The Role of Microbiota in Gastric Cancer: A Comprehensive Review," *Helicobacter* 29, no. 2 (2024): e13071.

2. Y. Y. Cheok, C. Y. Q. Lee, H. C. Cheong, et al., "An Overview of *Helicobacter pylori* Survival Tactics in the Hostile Human Stomach Environment," *Microorganisms* 9, no. 12 (2021): 2502.

3. K. M. Ottemann and A. C. Lowenthal, "*Helicobacter pylori* Uses Motility for Initial Colonization and to Attain Robust Infection," *Infection and Immunity* 70, no. 4 (2002): 1984–1990.

4. H. Singh, A. Ye, and M. J. Ferrua, "Aspects of Food Structures in the Digestive Tract," *Current Opinion in Food Science* 3 (2015): 85–93.

5. A. Danielli, G. Amore, and V. Scarlato, "Built Shallow to Maintain Homeostasis and Persistent Infection: Insight Into the Transcriptional Regulatory Network of the Gastric Human Pathogen *Helicobacter pylori*," *PLoS Pathogens* 6, no. 6 (2010): e1000938.

6. P. Lertsethtakarn, K. M. Ottemann, and D. R. Hendrixson, "Motility and Chemotaxis in *Campylobacter* and *Helicobacter*," *Annual Review of Microbiology* 65 (2011): 389–410.

7. E. Niehus, H. Gressmann, F. Ye, et al., "Genome-Wide Analysis of Transcriptional Hierarchy and Feedback Regulation in the Flagellar System of *Helicobacter pylori*," *Molecular Microbiology* 52, no. 4 (2004): 947–961.

8. F. Konig, S. L. Svensson, and C. M. Sharma, "Interplay of Two Small RNAs Fine-Tunes Hierarchical Flagella Gene Expression in *Campylobacter jejuni*," *Nature Communications* 15, no. 1 (2024): 5240.

9. D. Roncarati, E. Pinatel, E. Fiore, C. Peano, S. Loibman, and V. Scarlato, "*Helicobacter pylori* Stress-Response: Definition of the HrcA Regulon," *Microorganisms* 7, no. 10 (2019): 436, https://doi.org/10.3390/microorganisms7100436.

10. S. Pepe, E. Pinatel, E. Fiore, et al., "The *Helicobacter pylori* Heat-Shock Repressor HspR: Definition of Its Direct Regulon and Characterization of the Cooperative DNA-Binding Mechanism on Its Own Promoter," *Frontiers in Microbiology* 9 (2018): 1887.

11. A. Vannini, D. Roncarati, and A. Danielli, "The *cag*-Pathogenicity Island Encoded CncR1 sRNA Oppositely Modulates *Helicobacter pylori* Motility and Adhesion to Host Cells," *Cellular and Molecular Life Sciences* 73, no. 16 (2016): 3151–3168.

12. C. Y. Kao, B. S. Sheu, and J. J. Wu, "*Helicobacter pylori* Infection: An Overview of Bacterial Virulence Factors and Pathogenesis," *Biomed J* 39, no. 1 (2016): 14–23.

13. J. A. Fields, J. Li, C. J. Gulbronson, D. R. Hendrixson, and S. A. Thompson, "*Campylobacter jejuni* CsrA Regulates Metabolic and Virulence Associated Proteins and is Necessary for Mouse Colonization," *PLoS One* 11, no. 6 (2016): e0156932.

14. G. Dugar, S. L. Svensson, T. Bischler, et al., "The CsrA-FliW Network Controls Polar Localization of the Dual-Function Flagellin mRNA in *Campylobacter jejuni*," *Nature Communications* 7 (2016): 11667.

15. J. Tsang and T. R. Hoover, "Basal Body Structures Differentially Affect Transcription of RpoN- and FliA-Dependent Flagellar Genes in *Helicobacter pylori*," *Journal of Bacteriology* 197, no. 11 (2015): 1921–1930.

16. C. Y. Kao, B. S. Sheu, and J. J. Wu, "CsrA Regulates *Helicobacter pylori* J99 Motility and Adhesion by Controlling Flagella Formation," *Helicobacter* 19, no. 6 (2014): 443–454.

17. J. A. Fields and S. A. Thompson, "*Campylobacter jejuni* CsrA Complements an *Escherichia coli csrA* Mutation for the Regulation of Biofilm Formation, Motility and Cellular Morphology but Not Glycogen Accumulation," *BMC Microbiology* 12 (2012): 233.

18. F. M. Barnard, M. F. Loughlin, H. P. Fainberg, et al., "Global Regulation of Virulence and the Stress Response by CsrA in the Highly Adapted Human Gastric Pathogen *Helicobacter pylori*," *Molecular Microbiology* 51, no. 1 (2004): 15–32.

19. C. Pourciau, Y. J. Lai, M. Gorelik, P. Babitzke, and T. Romeo, "Diverse Mechanisms and Circuitry for Global Regulation by the RNA-Binding Protein CsrA," *Frontiers in Microbiology* 11 (2020): 601352.

20. A. H. Potts, C. A. Vakulskas, A. Pannuri, H. Yakhnin, P. Babitzke, and T. Romeo, "Global Role of the Bacterial Post-Transcriptional Regulator CsrA Revealed by Integrated Transcriptomics," *Nature Communications* 8, no. 1 (2017): 1596.

21. B. L. Wei, A. M. Brun-Zinkernagel, J. W. Simecka, B. M. Pruss, P. Babitzke, and T. Romeo, "Positive Regulation of Motility and *flhDC* Expression by the RNA-Binding Protein CsrA of *Escherichia coli*," *Molecular Microbiology* 40, no. 1 (2001): 245–256.

22. H. Yakhnin, P. Pandit, T. J. Petty, C. S. Baker, T. Romeo, and P. Babitzke, "CsrA of *Bacillus subtilis* Regulates Translation Initiation of the Gene Encoding the Flagellin Protein (*hag*) by Blocking Ribosome Binding," *Molecular Microbiology* 64, no. 6 (2007): 1605–1620.

23. C. A. Vakulskas, Y. Leng, H. Abe, et al., "Antagonistic Control of the Turnover Pathway for the Global Regulatory sRNA CsrB by the CsrA and CsrD Proteins," *Nucleic Acids Research* 44, no. 16 (2016): 7896–7910.

24. C. A. Vakulskas, A. H. Potts, P. Babitzke, B. M. Ahmer, and T. Romeo, "Regulation of Bacterial Virulence by Csr (Rsm) Systems," *Microbiology and Molecular Biology Reviews* 79, no. 2 (2015): 193–224.

25. T. Weilbacher, K. Suzuki, A. K. Dubey, et al., "A Novel sRNA Component of the Carbon Storage Regulatory System of *Escherichia coli*," *Molecular Microbiology* 48, no. 3 (2003): 657–670.

26. T. Romeo, "Global Regulation by the Small RNA-Binding Protein CsrA and the Non-Coding RNA Molecule CsrB," *Molecular Microbiology* 29, no. 6 (1998): 1321–1330.

27. M. Y. Liu, G. Gui, B. Wei, et al., "The RNA Molecule CsrB Binds to the Global Regulatory Protein CsrA and Antagonizes Its Activity in *Escherichia coli*," *Journal of Biological Chemistry* 272, no. 28 (1997): 17502–17510.

28. F. Ye, F. Yang, R. Yu, et al., "Molecular Basis of Binding Between the Global Post-Transcriptional Regulator CsrA and the T3SS Chaperone CesT," *Nature Communications* 9, no. 1 (2018): 1196.

29. R. T. Oshiro, S. Rajendren, H. A. Hundley, and D. B. Kearns, "Robust Stoichiometry of FliW-CsrA Governs Flagellin Homeostasis and Cytoplasmic Organization in *Bacillus subtilis*," *mBio* 10, no. 3 (2019): e00533.

30. K. A. Radomska, M. Wosten, S. R. Ordonez, J. A. Wagenaar, and J. P. M. van Putten, "Importance of *Campylobacter jejuni* FliS and FliW in Flagella Biogenesis and Flagellin Secretion," *Frontiers in Microbiology* 8 (2017): 1060.

31. S. Mukherjee, R. T. Oshiro, H. Yakhnin, P. Babitzke, and D. B. Kearns, "FliW Antagonizes CsrA RNA Binding by a Noncompetitive Allosteric Mechanism," *Proceedings of the National Academy of Sciences of the United States of America* 113, no. 35 (2016): 9870–9875.

32. K. Y. Yang, C. Y. Kao, M. S. Su, et al., "Glycosyltransferase Jhp0106 (PseE) Contributes to Flagellin Maturation in *Helicobacter pylori*," *Helicobacter* 26, no. 2 (2021): e12787.

33. M. W. Pfaffl, "A New Mathematical Model for Relative Quantification in Real-Time RT-PCR," *Nucleic Acids Research* 29, no. 9 (2001): e45.

34. K. Katoh and D. M. Standley, "MAFFT Multiple Sequence Alignment Software Version 7: Improvements in Performance and Usability," *Molecular Biology and Evolution* 30, no. 4 (2013): 772–780.

35. K. P. Schliep, "Phangorn: Phylogenetic Analysis in R," *Bioinformatics* 27, no. 4 (2011): 592–593.

36. M. Mirdita, K. Schutze, Y. Moriwaki, L. Heo, S. Ovchinnikov, and M. Steinegger, "ColabFold: Making Protein Folding Accessible to all," *Nature Methods* 19, no. 6 (2022): 679–682.

37. C. J. Wu, Y. Chen, L. H. Li, et al., "Roles of SmeYZ, SbiAB, and SmeDEF Efflux Systems in Iron Homeostasis of *Stenotrophomonas maltophilia*," *Microbiology Spectrum* 10, no. 3 (2022): e0244821.

38. R. T. Oshiro, C. M. Dunn, and D. B. Kearns, "Contact With the CsrA Core is Required for Allosteric Inhibition by FliW in *Bacillus subtilis*," *Journal of Bacteriology* 203, no. 2 (2020): e00574.

39. F. Altegoer, S. A. Rensing, and G. Bange, "Structural Basis for the CsrA-Dependent Modulation of Translation Initiation by an Ancient Regulatory Protein," *Proceedings of the National Academy of Sciences of the United States of America* 113, no. 36 (2016): 10168–10173.

40. S. R. Pernitzsch, M. Alzheimer, B. U. Bremer, M. Robbe-Saule, H. De Reuse, and C. M. Sharma, "Small RNA Mediated Gradual Control of Lipopolysaccharide Biosynthesis Affects Antibiotic Resistance in *Helicobacter pylori*," *Nature Communications* 12, no. 1 (2021): 4433.

41. R. Kinoshita-Daitoku, K. Kiga, M. Miyakoshi, et al., "A Bacterial Small RNA Regulates the Adaptation of *Helicobacter pylori* to the Host Environment," *Nature Communications* 12, no. 1 (2021): 2085.

42. S. R. Pernitzsch, S. M. Tirier, D. Beier, and C. M. Sharma, "A Variable Homopolymeric G-Repeat Defines Small RNA-Mediated Posttranscriptional Regulation of a Chemotaxis Receptor in *Helicobacter pylori*," *Proceedings of the National Academy of Sciences of the United States of America* 111, no. 4 (2014): E501–E510.

43. C. Y. Kao, J. W. Chen, S. Wang, B. S. Sheu, and J. J. Wu, "The *Helicobacter pylori* J99 *jhp0106* Gene, Under the Control of the CsrA/RpoN Regulatory System, Modulates Flagella Formation and Motility," *Frontiers in Microbiology* 8 (2017): 483.

Supporting Information

Additional supporting information can be found online in the Supporting Information section.